

# UC Davis

## UC Davis Previously Published Works

### Title

A pivotal role for starch in the reconfiguration of  $^{14}\text{C}$ -partitioning and allocation in *Arabidopsis thaliana* under short-term abiotic stress.

### Permalink

<https://escholarship.org/uc/item/3q23d5rh>

### Journal

Scientific reports, 8(1)

### ISSN

2045-2322

### Authors

Dong, Shaoyun  
Zhang, Joshua  
Beckles, Diane M

### Publication Date

2018-06-01

### DOI

10.1038/s41598-018-27610-y

Peer reviewed

# SCIENTIFIC REPORTS

OPEN

## A pivotal role for starch in the reconfiguration of $^{14}\text{C}$ -partitioning and allocation in *Arabidopsis thaliana* under short-term abiotic stress

Shaoyun Dong, Joshua Zhang & Diane M. Beckles 

Plant carbon status is optimized for normal growth but is affected by abiotic stress. Here, we used  $^{14}\text{C}$ -labeling to provide the first holistic picture of carbon use changes during short-term osmotic, salinity, and cold stress in *Arabidopsis thaliana*. This could inform on the early mechanisms plants use to survive adverse environment, which is important for efficient agricultural production. We found that carbon allocation from source to sinks, and partitioning into major metabolite pools in the source leaf, sink leaves and roots showed both conserved and divergent responses to the stresses examined. Carbohydrates changed under all abiotic stresses applied; plants re-partitioned  $^{14}\text{C}$  to maintain sugar levels under stress, primarily by reducing  $^{14}\text{C}$  into the storage compounds in the source leaf, and decreasing  $^{14}\text{C}$  into the pools used for growth processes in the roots. Salinity and cold increased  $^{14}\text{C}$ -flux into protein, but as the stress progressed, protein degradation increased to produce amino acids, presumably for osmoprotection. Our work also emphasized that stress regulated the carbon channeled into starch, and its metabolic turnover. These stress-induced changes in starch metabolism and sugar export in the source were partly accompanied by transcriptional alteration in the T6P/SnRK1 regulatory pathway that are normally activated by carbon starvation.

Plants are the primary producers on earth, assimilating carbon dioxide by daytime photosynthesis for the biogenesis of all essential structures. This carbon assimilate is *partitioned* primarily into sugars and starch in the autotrophic ‘sources’<sup>1</sup> with a portion of the sugars *allocated* to the heterotrophic ‘sinks’ to support growth of the latter<sup>1</sup>. In the absence of photoassimilation, the starch stored in the source is degraded to replenish cellular sugars in order to avoid carbon starvation<sup>2–5</sup>. Therefore, carbon assimilation and utilization is carefully balanced for optimal plant development.

Adverse environmental conditions can disrupt the normal starch and sugars levels with repercussions for the ability of the plant to sustain growth<sup>6</sup>. Drought is associated with reduced starch or sugar levels in source tissues<sup>7–11</sup>. Salinity stress can induce higher starch accumulation in the source or sink of some species<sup>12–17</sup>, but trigger starch reduction in others<sup>18,19</sup>. Similarly, chilling stress is associated with accelerated source-starch accumulation<sup>20–22</sup> or degradation<sup>23–25</sup>. These observed increases in starch or sugars may be adaptive responses for stress-survival<sup>6</sup>, or may be ‘injury’ responses resulting from the under-utilization of carbon because of growth cessation<sup>26,27</sup>, regardless, documenting these changes is necessary for a deeper understanding of plant stress response.

Feeding plants with  $^{14}\text{CO}_2$  is useful for tracking carbon movement, and can inform on changes in carbon allocation due to stress<sup>17,28–34</sup>. Available data suggests that stress generally accelerates allocation to the sinks as an adaptive response<sup>35</sup>. Salinity increased flux from source to developing fruits in tomato<sup>36</sup> and to the roots in transgenic rice seedlings<sup>17</sup>. Water-stress elicited a similar distribution pattern in (a) *Arabidopsis*, with higher  $^{14}\text{C}$  allocated to the roots<sup>30</sup>, (b) in beans, where  $^{14}\text{C}$  flux to the pods increased<sup>8</sup>, and (c) in rice, where it stimulated  $^{14}\text{C}$

Department of Plant Sciences, University of California, One Shield Avenue, Davis, CA, 95616, USA. Correspondence and requests for materials should be addressed to D.M.B. (email: [dbeckles@ucdavis.edu](mailto:dbeckles@ucdavis.edu))

mobilization from the stem and allocation to the grain<sup>37</sup>. Additional  $^{14}\text{C}$ -allocation studies under varied stress conditions could help to clarify whether or not higher source-sink flux is a universal stress response.

The observed changes in local and distant carbon fluxes in plant tissues during stress result from multiple activities – epigenetic, transcriptional, post-transcriptional and posttranslational changes, occurring across different spatial and temporal scales, which must be integrated to deliver a cohesive response to stress<sup>38–42</sup>. The trehalose-6-phosphate/Sucrose non-Fermented Related Kinase 1 (T6P/SnRK1) signaling cascade<sup>40</sup> may function in this way. It is critical for plant survival under low carbon and energy conditions<sup>43</sup>, in part through changes in starch metabolism<sup>44,45</sup>. The T6P/SnRK1 can also modulate source-sink interactions; therefore, key elements of this regulatory network could potentially be activated for a ‘rewiring’ of whole plant carbohydrate use under stress.

Because of the many issues with respect to plant carbon use under stress that remain unresolved, our aim in this work was to investigate changes in carbon partitioning and allocation in response to short-term drought, salinity, and cold stresses.  $^{14}\text{CO}_2$ -labeling of a single source leaf<sup>28</sup> was used to map whole-plant and intra-tissue changes in carbon use, as it can provide partitioning and allocation data in the same system. Single-leaf labeling permits more accurate tracking of  $^{14}\text{C}$ -movement than can be obtained by exposing the entire rosette to the label<sup>28</sup>. By comparing plants exposed to different stresses it may be possible to identify convergent and divergent adaptive responses associated with each unfavorable condition. Starch content was also assayed in the source leaf and the roots of the stressed plants and the data were compared to  $^{14}\text{C}$ -starch fluxes to identify how starch metabolism may be regulated to alter sugar distribution. Finally, the transcriptional activity of key genes in the T6P/SnRK1 pathway was assessed to identify genes associated with changes in carbohydrate levels under abiotic stress. By integrating these data, we present one of the first comprehensive pictures of how *Arabidopsis* changes carbon flux under short-term environmental stress. This information could be combined with that generated from the wealth of -omics data to broaden our understanding of plant stress response.

## Results

**Time course changes of carbon partitioning and allocation in non-stress treated plants.** Our first aim was to investigate how plant source and sink tissues use carbon over the diurnal cycle under normal conditions. One hour before the middle of the day (MD), a single mature, but still developing source leaf was fed with  $^{14}\text{CO}_2$  for 5 min. The labeled source leaf, unlabeled sink leaves, and the roots were harvested separately at MD, at the end of the day (ED), and at the end of the night (EN). MD, ED and EN correspond to 6 h, 12 h and 24 h after dawn. The percentage of  $^{14}\text{C}$  distributed among the source and the sinks was determined. Within each tissue, the incorporation of  $^{14}\text{C}$  into the main metabolites pools: sugars, amino acids, organic acids, starch, protein, and ‘remaining insoluble compounds’ (RICs), was established.

First, we calculated the percentage of  $^{14}\text{C}$  distributed from the source to the sinks. During the day, ~60% of the  $^{14}\text{C}$  was retained in the source leaf, but by EN, the percentage of total  $^{14}\text{C}$  was evenly distributed (30%) among all tissues (Fig. 1A). Nighttime export of  $^{14}\text{C}$  from the source, and its subsequent allocation into the sinks, accounted for the re-distribution.

Second, we examined the  $^{14}\text{C}$  partitioning between the source and sinks (Figs 1B, 2A) to create a full picture of how allocation and subsequent partitioning were altered. Partitioning in the roots was more dynamic than in the sink leaves, and this difference was amplified most at ED (Fig. 2A). In the roots, there was increased incorporation of  $^{14}\text{C}$  into metabolites used for growth — i.e. sugars, amino acids, and RICs — and less into those used for storage — i.e. protein and starch — compared to the source. The pattern of  $^{14}\text{C}$ -partitioning in source leaf vs. roots therefore reflected the prioritization of biological processes in each tissue type. The other change of note occurred at EN, when both sinks incorporated less  $^{14}\text{C}$  into organic acids but more into starch compared to the source. This may indicate that the sinks had greater sufficiency with respect to carbon (due to sugar import) with a relatively reduced need for organic acids as sources of energy compared to the source.

Finally, we examined changes in  $^{14}\text{C}$ -partitioning over the diurnal cycle (Fig. 2B). Data at ED and EN were compared to that generated at MD to fully assess how the day-night cycle affected carbon partitioning in different tissues. The metabolic pools in the source leaf were variable, while those in the sinks were relatively stable. Relative to MD, there was less  $^{14}\text{C}$  in the sugar and starch fraction, but an almost 2-fold greater flux into organic acids at EN in the source. Organic acids may serve as the primary substrate for respiration after reductions in the sugar pool<sup>1</sup>. In the roots, at EN, the  $^{14}\text{C}$  percentage in sugars decreased, but increased in starch. This indicates that the starch in the roots was accumulated constantly during the diurnal cycle, with more accretion during the night than the day. In contrast, in the sink leaves, the carbon flow into sugars and starch were stable at EN, but there was a 4-fold increase in the  $^{14}\text{C}$  partitioned into the RICs, suggestive of nighttime growth processes.

**Carbon partitioning and allocation under abiotic stress.** How stress altered *Arabidopsis* carbon use over the diurnal cycle at the cellular and whole plant level was examined. *Arabidopsis* seedlings were exposed to salinity stress using 100 and 200 mM NaCl, to osmotic stress using 150 and 300 mM mannitol, and to cold stress by exposing roots to 0 °C cold at the beginning of photoperiod. After 5 hours of stress treatment, a single mature source leaf was fed with  $^{14}\text{CO}_2$  for 5 min. Sampling was done as previously described.

**Osmotic stress.** Carbon allocation was negatively affected by osmotic stress, and the inhibition grew in severity as the stress progressed (see Supplementary Fig. S1). By EN, mild (150 mM) and severe (300 mM) mannitol stress increased the percentage of  $^{14}\text{C}$  in the source, and decreased it in the roots (see Supplementary Fig. S1). This could reflect reduced carbon export due to enhanced source activities, inhibited carbon export from the source, reduced sink strength, or a combination thereof under osmotic stress.

Carbon partitioning within the source was also modulated to a greater extent than in the sinks (Fig. 3). At MD, both mild and severe osmotic stress reduced the  $^{14}\text{C}$ -partitioned into starch but increased  $^{14}\text{C}$ -partitioning into organic acids in the source, presumably for respiratory use. Six hours later, only severe osmotic stress had this

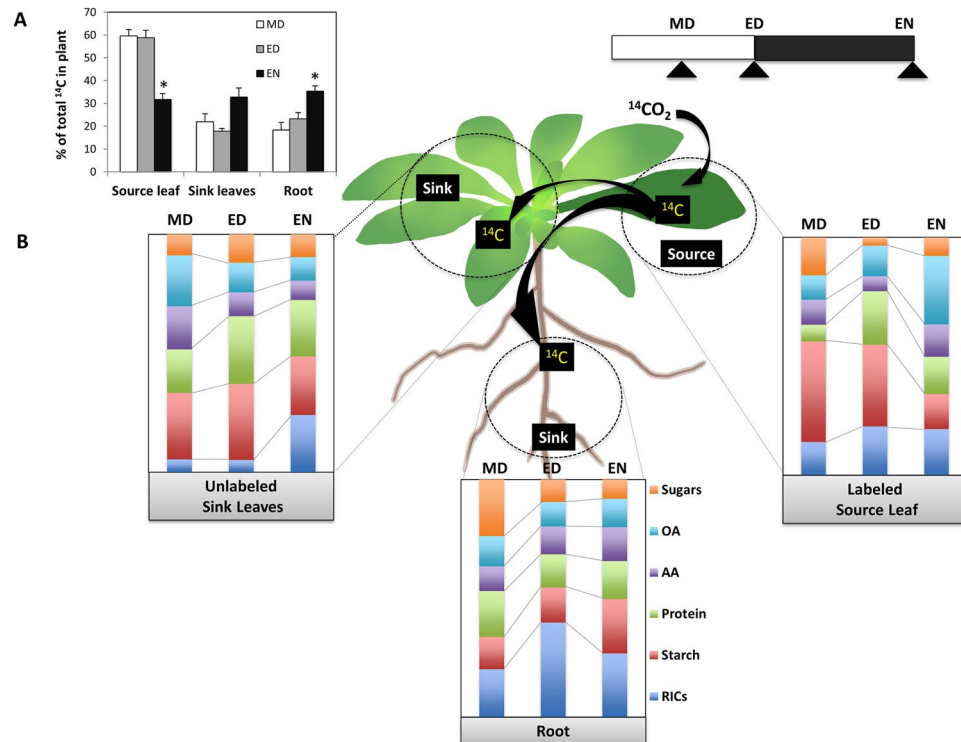


**Figure 1.** Carbon allocation and partitioning under control conditions. **(A)** Percentage of  $^{14}\text{C}$  allocated from the labeled source leaf to unlabeled sink leaves and root. The relative amount of  $^{14}\text{C}$  in each tissue was shown as a percentage of total label in the whole plant. **(B)** Percentage of  $^{14}\text{C}$  partitioning into metabolite pools. The total  $^{14}\text{C}$  incorporated into the sugars, starch, amino acids (AA), proteins, organic acids (OA), and remaining insoluble compounds (RICs) in each tissue was set to 100%. MD: midday, ED: end of day, EN: end of night.

effect leading to greater  $^{14}\text{C}$  flux into osmoprotectants — sugars, organic acids, and amino acids — at the expense of the storage compounds (i.e. starch). The  $^{14}\text{C}$ -flux into these osmoprotectants also increased in both sinks at the expense of the RICs, with the latter decreasing drastically (by 34.7% at ED and 14.3% at EN) in the roots.

**Salinity stress.** The most obvious change was the percentage of  $^{14}\text{C}$  allocated from source leaf into roots, which decreased significantly by EN under both mild (100 mM) and severe (200 mM) NaCl stress (see Supplementary Fig. S2). The  $^{14}\text{C}$ -use in source leaf was more responsive to salinity compared to the sinks (Fig. 4). Severe salinity stress decreased  $^{14}\text{C}$ -partitioning into starch but increased partitioning into sugars, amino acids, and organic acids during the day in the source. At MD, more  $^{14}\text{C}$  was partitioned into sugars in the sink leaves, but 6 h later at ED the  $^{14}\text{C}$  in sugars was stable, with reduced flux into starch and proteins. This indicates that 12 h after the stress treatment, carbon was diverted from storage and preferentially partitioned into sugars for osmoprotection. In the roots, less  $^{14}\text{C}$  was partitioned into the RICs at ED and EN compared to the control, which suggest a shift away from investing  $^{14}\text{C}$  into resources normally used for root growth under salinity. This may have led to increased  $^{14}\text{C}$  accumulation into sugars at the end of night because they were under-metabolized. Interestingly, proteins were the only metabolite affected by both mild and severe salinity stress in both source and sink leaves, while it was unchanged in the roots. Carbon flux into this pool decreased compared to the control at ED in both source and sink leaves. Further, unlike sink leaves, the source had increased  $^{14}\text{C}$  label in protein at MD (Fig. 4).

The changes in  $^{14}\text{C}$  partitioning and allocation in response to different levels of salinity stress are summarized as follows: (a) the source leaf partitioned less  $^{14}\text{C}$  into storage compounds (starch, or protein) but more  $^{14}\text{C}$  into osmoprotectants (sugars, amino acids, organic acids) in response to severe salinity stress; (b) sink tissues showed a differential response to salinity stress: similar to the source leaf, the sink leaves showed reduced  $^{14}\text{C}$  in storage compounds, however, roots tissue had reduced  $^{14}\text{C}$  in structural compounds; and (c) the amount of  $^{14}\text{C}$  imported into roots tissue was inhibited by salinity; this might be due to reduced sink activity, inhibited phloem transport, or a combination thereof.

**Cold stress.** The percentage of  $^{14}\text{C}$  in root tissues was significantly reduced by cold stress at the end of night, showing similarity to tissues under osmotic and salinity stress (see Supplementary Fig. S3). Carbon allocation was not affected by low temperature during the day (see Supplementary Fig. S3), but carbon partitioning was highly regulated in the source leaf (Fig. 5), especially at the end of day. The most notable difference was that the  $^{14}\text{C}$ -flux into starch and RICs decreased relative to the control plants. The decrease in starch was high at MD but lessened during the diurnal cycle, while the opposite was true for the RICs, where inhibition intensified over the day. In the source, there were also higher fluxes into sugars, amino acids, and organic acids from MD to ED. Cold

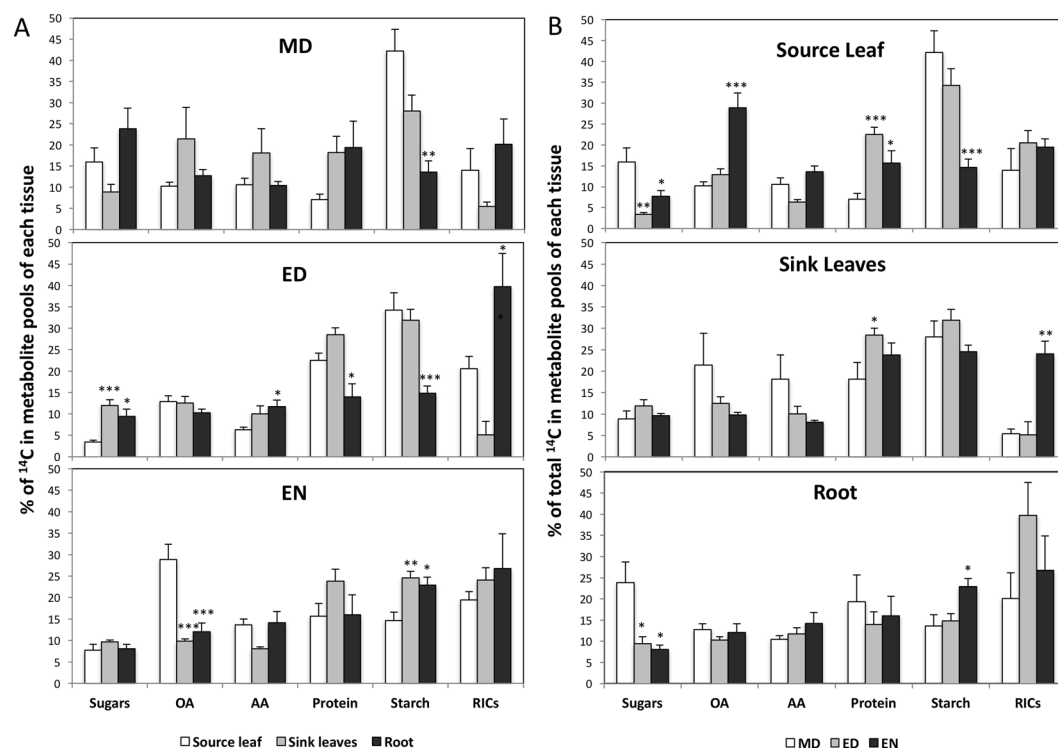


**Figure 2.** The changes in carbon partitioning over time in different tissues. (A). The percentage difference in <sup>14</sup>C within the metabolite pools among tissues. The asterisks indicate a significant difference between the source leaf and either the sink leaves or root. (B) The differential percentage of <sup>14</sup>C in metabolite pools over time. The asterisks indicate a significant difference between the midday (MD) and end of day (ED) or end of night (EN). The total <sup>14</sup>C partitioned into sugars, organic acids (OA), amino acids (AA), protein, starch, and remaining insoluble compounds (RICs) in each tissue was set to 100%. (n = 5, \* $0.01 < p < 0.05$ ; \*\* $0.001 < p < 0.01$ ; \*\*\* $0 < p < 0.001$ ).

also triggered increased <sup>14</sup>C into the protein pool at MD, and decreased it at ED. At EN, the <sup>14</sup>C in RICs strongly decreased, with a corresponding strong increase in sugars. Cold stress therefore stimulated more <sup>14</sup>C partitioning into sugars over the diurnal cycle in the source leaf.

The sinks were less affected by cold than the source. In sink leaves, there was increased carbon flow into sugars during the day and decreased carbon into starch at night, with no difference in RICs. In contrast, the roots had increased <sup>14</sup>C in the sugar pool at night, and reduced partitioning into the RICs (at ED by 20.4% and at EN by 11.6%). This change of <sup>14</sup>C partitioning suggests reprioritization of reserves with a greater flux towards sugars for osmoprotection at the expense of other pathways.

**Steady-state accumulation of starch vs. partitioning under abiotic stress.** The <sup>14</sup>CO<sub>2</sub> labeling experiment showed that starch is the most dynamic metabolite pool that changed under all types of abiotic stresses used in this study. <sup>14</sup>C-flux into starch was down-regulated by abiotic stress, and the regulation depended on the time of day and tissue type examined.

Under control conditions, <sup>14</sup>C-partitioning into starch was stable during the day but decreased at night in the source leaf (see Supplementary Fig. 7A). However, this pattern was disrupted under salinity and cold stress due to reduced carbon flow into starch. In contrast to the source leaf, <sup>14</sup>C in starch in sink leaves did not change during the day even under stress. In roots, the percentage of <sup>14</sup>C into starch normally increased by EN, and interestingly, this partitioning was maintained under osmotic stress, but not under salinity and cold stress. Source and sink tissues therefore partitioned carbon into starch differently in response to abiotic stress (see Supplementary Fig. 7B). Source leaf showed reduced <sup>14</sup>C partitioning into starch at MD under both mild and severe salinity and osmotic stress, and at ED under severe stress only. Sink tissues had very little changes of <sup>14</sup>C in starch under stress.

Since the plants were labeled 5 h after the stress treatment, the <sup>14</sup>C flux into starch cannot provide a whole picture of starch metabolism changes during the entire stress period. It only informs on percentage change in partitioning and allocation. Therefore, absolute starch content measurements were made in source leaf and roots (Fig. 6), to determine changes in accumulation over the time-course. Comparison of the variations in the percentage of <sup>14</sup>C partitioned into starch with changes in starch accumulation could indicate if there are additional regulatory mechanisms leading to turnover, i.e. simultaneous synthesis and degradation.

Cold, mild osmotic and salinity stress triggered enhanced starch accumulation at ED in the source. Twelve hours later (EN), only cold and mild salinity kept starch accumulation high relative to the non-stressed control. In comparison, the <sup>14</sup>C that partitioned into starch decreased from ED to EN (see Supplementary Fig. 7A), thus, the increased starch content observed might be due to inhibited starch degradation early in the day. A similar pattern was found

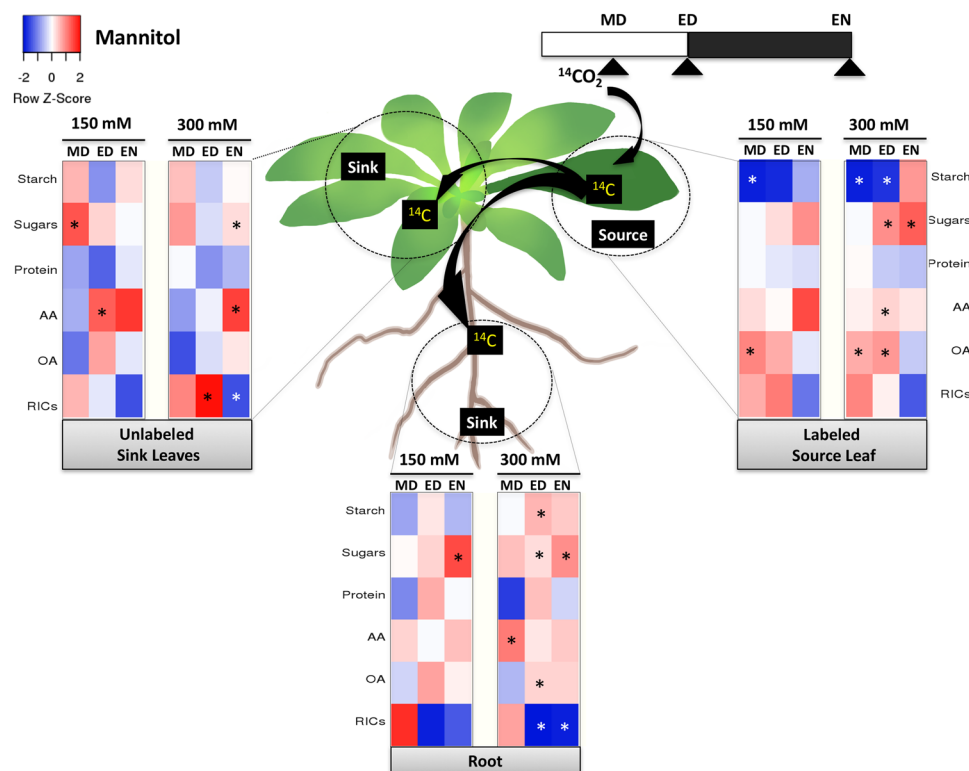


**Figure 3.** A diagram showing changes in  $^{14}\text{C}$  partitioning within each tissue under osmotic stress. Heat map showing the difference in  $^{14}\text{C}$  partitioning over time between the stress-treated samples and control. The incorporation of  $^{14}\text{C}$  into sugars, starch, amino acids (AA), protein, organic acids (OA), and remaining insoluble compounds (RICs) pools in each tissue was set to 100%. The difference in  $^{14}\text{C}$  percentage between mannitol-treated (150 or 300 mM) and control in each metabolite was calculated, and the differences were shown as a heat map. Red represents a higher percentage than the control, while blue represents a lower percentage than the control. The asterisk indicates a significant difference between the control and mannitol-treated plants ( $n = 5$ ,  $p < 0.05$ ). MD: midday, ED: end of day, EN: end of night.

in the roots — higher starch accumulation even though there was no change in the percentage of  $^{14}\text{C}$  partitioned to starch over the same period. Therefore stress may have reduced the rate of starch turnover in the roots.

**Transcript level of genes integrate carbohydrate and abiotic stress.** Because the starch-sugar inter-conversion in source leaf was acutely regulated in response to environmental cues, we further examined if changes in starch metabolism and sugar export was accompanied by the regulation of the known T6P/SnRK1 stress signaling pathway genes. The transcript level of five selected genes in source leaf exposed to 300 mM mannitol and 200 mM NaCl stress, which triggered the most dynamic changes in starch metabolism, were evaluated. These genes are involved in starch synthesis, sucrose transport, and are components of the T6P/SnRK1 stress signaling pathway. *AtTPS1* encodes trehalose-6-phosphate (T6P) synthase<sup>46</sup>, *AtSnRK1.1* and *AtSnRK1.2* encode two major isoforms of SnRK1<sup>39–42</sup>, the central players of the T6P/SnRK1 pathway. *AtAPL3* encodes the large subunit of ADP-glucose pyrophosphorylase (AGPase) that catalyzes the first committed step in starch biosynthesis. *AtSWEET11* encodes a transporter that exports sucrose from leaf mesophyll cells into the phloem for transport to sinks<sup>47–49</sup>.

Our measurements showed that *AtSnRK1.2* was up-regulated by osmotic and salinity stress after 6 hours of treatment (Fig. 7). However, the transcription of *AtTPS1* and *AtSnRK1.1* did not change. *AtSWEET11* was down regulated by severe osmotic stress at the end of day. *AtAPL3* was up-regulated at MD and at EN by 300 mM mannitol stress, and was up-regulated from ED to EN by 200 mM NaCl.

## Discussion

**Carbon allocation and partitioning is regulated by abiotic stress.** Our overall aim was to develop a comprehensive map of time-dependent changes in carbon allocation and partitioning, to see how these processes were affected under different stresses.

In our study, the  $^{14}\text{C}$  partitioning in source and different types of sinks (leaves, and roots) over the diurnal cycle was examined. Under control conditions,  $^{14}\text{C}$  distribution into different metabolic pools in source and sink tissue, followed expectation based on previous knowledge<sup>29</sup>. Source leaf, sink leaves and roots tissues showed different carbon partitioning, with most dynamism in the source. Most carbon in source leaf flowed into storage compounds (starch), and less flowed into structural compounds (e.g. cell walls) during the day. This result is similar to a previous study<sup>29</sup>. The roots also generally incorporated more carbon into RICs while sink leaves partitioned more into starch. This indicates a clear differentiation in carbon use between sink leaves and roots.



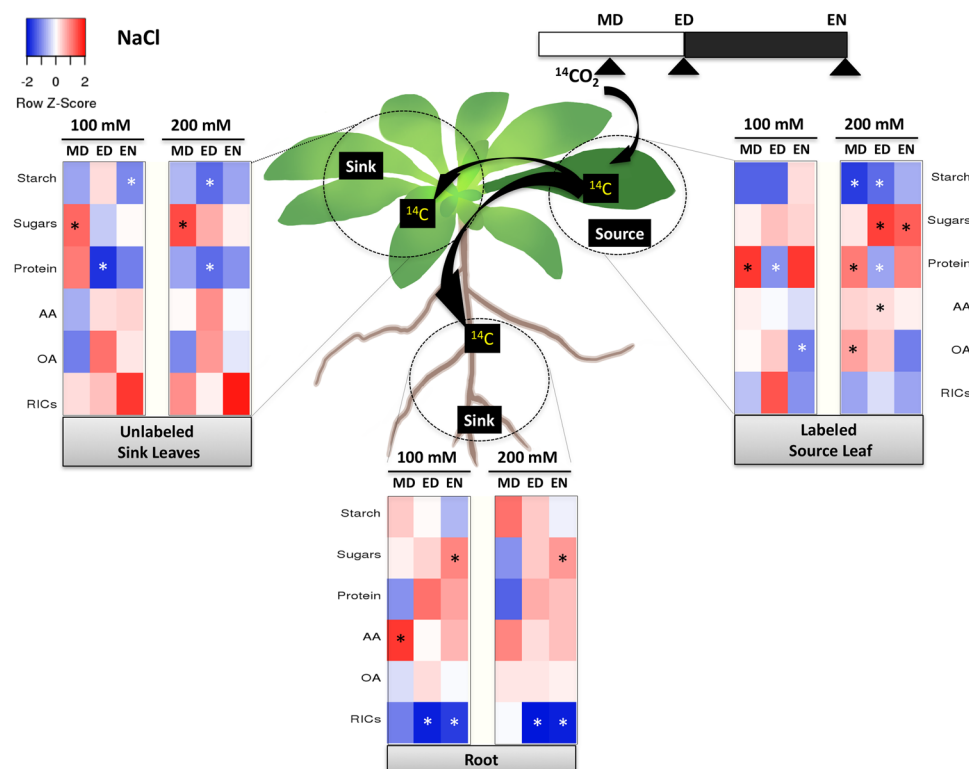


**Figure 4.** A diagram showing changes in  $^{14}\text{C}$  partitioning within each tissue under salinity stress. Heat map showing the difference in  $^{14}\text{C}$  partitioning over time between the stress-treated samples and control. The incorporation of  $^{14}\text{C}$  into sugars, starch, amino acids (AA), protein, organic acids (OA), and remaining insoluble compounds (RICs) pools in each tissue was set to 100%. The difference in  $^{14}\text{C}$  percentage between NaCl-treated (100 or 200 mM) and control in each metabolite was calculated, and the differences were shown as a heat map. Red represents a higher percentage than the control, while blue represents a lower percentage than the control. The asterisk indicates a significant difference between the control and NaCl-treated plants ( $n = 5$ ,  $p < 0.05$ ). MD: midday, ED: end of day, EN: end of night.

Carbon allocation to the sinks was modulated by all abiotic stress conditions used in our study (see Supplementary Figs S1–S3). Stress conditions should reduce photosynthetic capacity and carbon available for export. Knolling *et al.* showed that carbon export from the source to sink leaves was reduced in Arabidopsis experiencing dark-induced carbon-starvation<sup>29</sup>. Our study included roots, which is a stronger sink than leaves. We found that the C-fluxes into the roots were more vulnerable to stresses than those into sink leaves (see Supplementary Figs S1–S3). Furthermore, plants might regulate carbon allocation differently in response to long-term and short-term stresses requiring caution when making comparisons between studies. Durand *et al.*<sup>30</sup> observed a higher percentage of  $^{14}\text{C}$  allocated into roots in the long-term water deficit stressed Arabidopsis. However, data from plants exposed to short-term stress (24 h) in our study and plants exposed to a 16 h night<sup>29</sup> showed the opposite results: reduced percentage of  $^{14}\text{C}$  exported into roots. This underscores that timing, intensity, and type of stress regulate carbon allocation differently, even if some stresses show similar responses.

Osmotic, salinity, and cold stress all triggered complex changes in carbon partitioning and shared some commonalities (Fig. 8). All stresses increased the carbon partitioned into sugars in both source and sink tissues. They also decreased the  $^{14}\text{C}$  partitioning into starch in the source leaf while increasing organic acids and amino acids. Each stress had a more dramatic impact on source leaf than the sink tissues, with most changes occurring within the first 12 h of stress application. The abiotic stresses used here all triggered decreased  $^{14}\text{C}$  flux into RICs (the carbon pool representative of growth) in the roots (Figs 3–5). Among the major metabolites pools affected, changes of carbohydrates were most consistent. Kolling *et al.*<sup>29</sup> observed an increase of  $^{14}\text{C}$  into sugars and a reduction of  $^{14}\text{C}$  flux into the RICs pool in both source and sink leaves. However, in our study, the increased  $^{14}\text{C}$  flux into sugars in the source leaf was due to the re-partitioning of  $^{14}\text{C}$  from storage compound (i.e. starch), while the increase in the sink could be explained by the reduced  $^{14}\text{C}$  partitioning into structural compounds (i.e. cell walls).

Different abiotic stresses may uniquely regulate carbon use (Fig. 8). Only cold stress caused a decrease in  $^{14}\text{C}$  in RICs in source leaf. Osmotic and cold stress, but not salinity stress, increased  $^{14}\text{C}$  flux into organic acids and amino acids in root tissues, and enhanced  $^{14}\text{C}$  into amino acids in sink leaves. Only cold and salinity stress, provoked changes in  $^{14}\text{C}$  in protein in source and sink leaves. Higher  $^{14}\text{C}$  in protein at the early stage of the stress progression may be due to the accumulation of stress-responsive proteins and enzymes. When stress continued, storage compound like the storage, cytosolic, and vacuolar proteins are degraded and recycled to provide energy and substrates for respiration<sup>50–55</sup>.

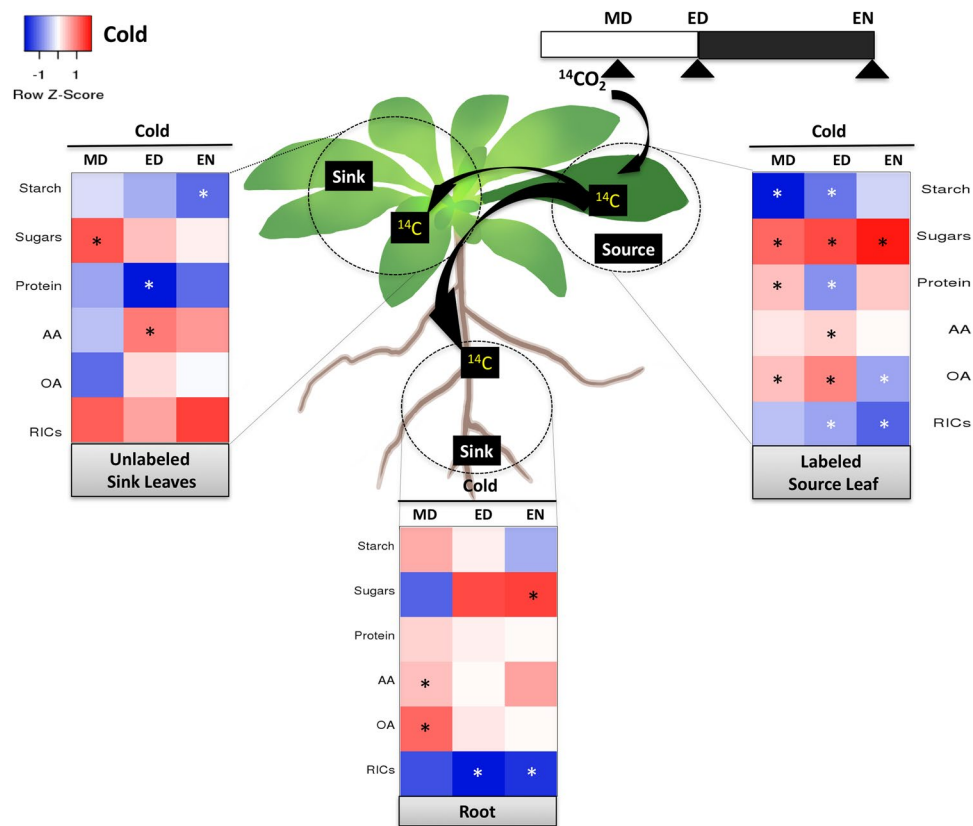


**Figure 5.** A diagram showing changes in  $^{14}\text{C}$  partitioning within each tissue under cold stress. Heat map showing the difference in  $^{14}\text{C}$  partitioning over time between the stress-treated samples and control. The incorporation of  $^{14}\text{C}$  into sugars, starch, amino acids (AA), protein, organic acids (OA), and remaining insoluble compounds (RICs) pools in each tissue was set to 100%. The difference in  $^{14}\text{C}$  percentage between cold-treated and control in each metabolite was calculated, and the differences were shown as a heat map. Red represents a higher percentage than the control, while blue represents a lower percentage than the control. The asterisk indicates a significant difference between the control and cold-treated plants ( $n = 5$ ,  $p < 0.05$ ). MD: midday, ED: end of day, EN: end of night.

**The regulation of starch metabolism in response to abiotic stress.** The regulation of starch accumulation by abiotic stress in Arabidopsis were mainly studied during the day and only focused on leaves. Mild-to-moderate mannitol stress (25 to 200 mM) triggered starch accumulation<sup>56–58</sup>, whereas higher mannitol concentrations (300 or 450 mM) or severe drought led to decreased leaf starch<sup>32,59–61</sup>. Moderate-to-severe salinity (150 mM NaCl) decreased starch in Arabidopsis leaves<sup>62</sup>. Cold stress induced starch accumulation in leaves in some studies<sup>20–22</sup>, while decreased starch accumulation in others<sup>23</sup>. Our study differentiated between source and sink tissues, and starch content was regulated by abiotic stress in both. There was a lack of congruency in the starch accumulation and  $^{14}\text{C}$ -starch partitioning under cold, mild osmotic, and salt stress in source and roots (Fig. 6 and Supplementary Fig. 7). Higher starch content in sink under stress might be due to decreased starch utilization. In the roots, more  $^{14}\text{C}$  accumulated as sugars because of the decreased  $^{14}\text{C}$  partitioning into structural compounds. In this case, it might not be necessary to degrade starch into sugars.

Starch, as a sugar reservoir, regulates plant carbon balance to avoid potential famine<sup>5,6,63–65</sup>. Maintaining sugar levels by cycles of synthesis and degradation of starch could permit metabolic flexibility with respect to starch-sugar interconversion. The sugars so produced may act as Reactive Oxygen Species scavengers, osmo-protectants and be an immediate source of carbon and energy to mitigate against stress<sup>66–70</sup>. Sugar conversion to starch in leaves may prevent feedback inhibition of photosynthesis, and higher starch in the roots could help gravitational response under stress, and enhance biomass for better foraging<sup>17,38</sup>.

**Transcript level of genes integrating carbohydrate and abiotic stress.** Transcripts levels of T6P/ SnRK1 pathway genes were regulated by abiotic stress in this study. *AtSWEET11*, one of the sucrose transporters, is important in whole-plant carbon allocation<sup>30,47,71</sup>. It is expressed when sucrose export is high<sup>30</sup> and repressed during osmotic stress in Arabidopsis leaves, when presumably export is lower<sup>71</sup>. In our study, *AtSWEET11* was down regulated by osmotic stress at the end of day, which suggests that the export of sugar to the sinks was inhibited. The repression was likely due to feedback inhibition by excess sugars, this is supported by our data, which showed more  $^{14}\text{C}$  in sugars in the source leaf at ED, and decreased  $^{14}\text{C}$  imported into roots (see Supplementary Fig. S2). *AtAPL3* was shown to be up-regulated by 150 mM NaCl stress in Arabidopsis<sup>62</sup>. Our study also observed the up-regulation of *AtAPL3* by 200 mM NaCl, and 300 mM mannitol stress. Interestingly, the percentage of



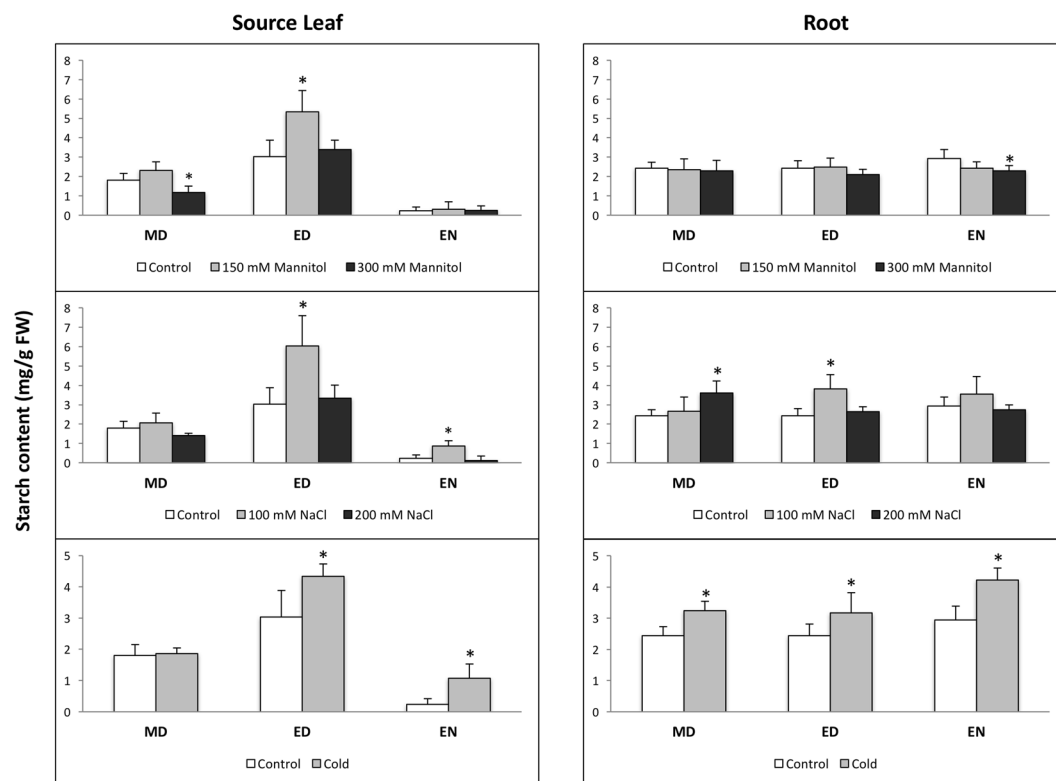


**Figure 6.** Starch contents in source leaf and root under stress. Starch was assayed in plants exposed to mannitol (150 or 300 mM), NaCl (100 or 200 mM), and cold stress for 6 h (MD: midday), 12 h (end of day), or 24 h (end of night). The asterisks indicate a significant difference between the stress-treated and control samples. MD: midday, ED: end of day, EN: end of night (n = 5,  $p < 0.05$ ).

$^{14}\text{C}$  partitioned into starch was reduced, and the end point starch content remained unchanged. Changes in the post-transcriptional regulation of AGPase rather than at the transcriptional level under stress may underscore starch contents assayed. SnRK1 has a pivotal role in regulating carbohydrate metabolism and resource partitioning under stress<sup>72,73</sup>. In this study, *AtSnRK1.2* was up-regulated by osmotic and salinity stress after 6 hours of stress treatment. However, the transcript of *AtTPS1* and *AtSnRK1.1* did not change, indicating a possible delayed response to stress compared with *AtSnRK1.2*. The inconsistency in transcript changes of *AtSnRK1.1* and *AtSnRK1.2* might also be due to the specificity of these isoforms in terms of spatial expression and function<sup>42,74</sup>. In maize, salinity stress triggered more starch and sugar accumulation in both source and sink tissues and the transcripts of the *ZmTPS1.1.1* and *ZmTPS1.2.1* genes in the source leaf were down-regulated, while SnRK1 target genes *AKINβ* was affected mainly in the sink but not in the source.

## Conclusion

The present study observed profound changes in whole plant carbon use as an early response to short-term abiotic stress in *Arabidopsis*. Stress induces a reconfiguration of plant carbon fluxes primarily through starch in the source and growth substance in the sinks. We identified common and divergent patterns of carbon use triggered by cold, salinity and osmotic stress. We also emphasized the role of starch metabolism in stress response via enhancing sugar flexibility, together with sugar efflux in the source leaf. The stress-induced carbohydrates alteration in source was associated with transcriptional changes of key genes in the carbon deficit activated T6P/SnRK1 signaling pathway. How carbon reconfiguration is triggered by the T6P/SnRK1 or other stress-responsive signaling pathways deserve future studies.

## Methods

**Growth Conditions and Stress Treatment.** *Arabidopsis thaliana* ecotype Colombia (Col-0) was grown hydroponically in Hoagland solution (12/12 h day/night, 21/23 °C). Five-week-old plants were transferred to Hoagland solution containing 100 mM NaCl, 200 mM NaCl, 150 mM mannitol, 300 mM mannitol, and 0 °C cold treatment for 5 hours before the  $^{14}\text{CO}_2$  labeling (n = 5).

**Starch content analysis.** Source leaf or roots tissue from each plant was ground to a fine powder, and boiled three times successively in 1.5 mL 80% (v/v) ethanol for 10 min each. The starch content was measured following the protocol previously used<sup>75</sup>; briefly, The pellet was dried briefly, and was digested into glucose with alpha-amylglucosidase and alpha-amylase (Roche Biosciences, Indianapolis, IN), then glucose content was measured at A340 nm absorbance and converted into starch content.

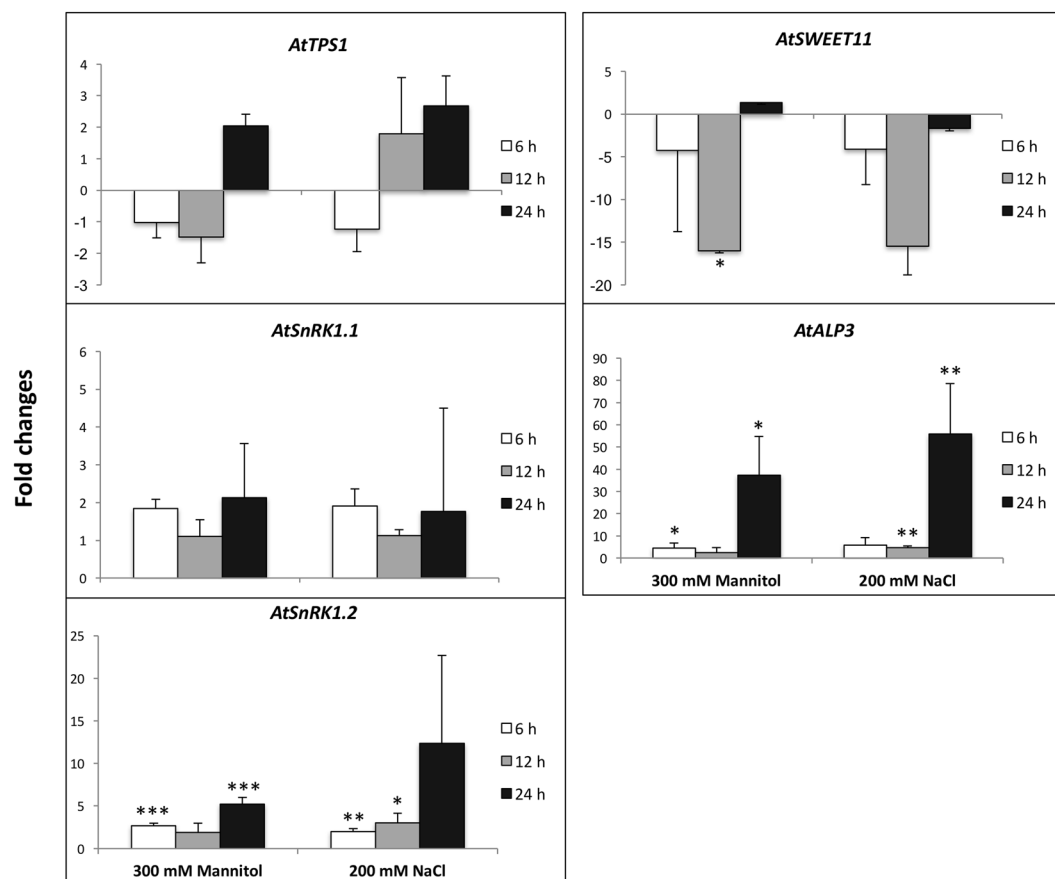


**Figure 7.** Quantification of transcripts from the *AtTPS1*, *AtSnRK1.1*, *AtSnRK1.2*, *AtSWEET11*, and *AtALP3* genes. The transcript levels of genes in non-stress treated control were set as 1. The vertical axis indicates the relative amount of mRNA of each gene in stress-treated samples compared with that in non-stress treated control. RNA samples were extracted from plants treated with 300 mM Mannitol or 200 mM NaCl for 6 h, 12 h, or 24 h. Average qPCR data were derived from nine data measurements for each sample. Error bars represent the standard deviation. The asterisks indicate statistically significant difference of transcripts level between genes in the control and stress-treated plants (\*,  $0.01 < p < 0.05$ ; \*\*,  $0.001 < p < 0.01$ ; \*\*\*,  $0 < p < 0.001$ ).

**$^{14}\text{CO}_2$  Pulse-Chase Labeling.** A single leaf  $^{14}\text{CO}_2$ -labeling device for *Arabidopsis* was modified based on the rice device<sup>17</sup> that was created following the prototype<sup>28</sup>. The  $^{14}\text{CO}_2$  feeding was carried out on the mature leaf of each twenty-leaf-old plant in the ‘leaf chamber’ in the middle of the photoperiod for 5 min.  $^{14}\text{CO}_2$  was generated from 0.08 MBq  $\text{NaH}^{14}\text{CO}_3$  acidified with 200  $\mu\text{L}$  of 10% (v/v) lactic acid in the reservoir chamber. The generated  $^{14}\text{CO}_2$  was pumped to a leaf chamber via the tubing system, where a single leaf of a plant was exposed to  $^{14}\text{CO}_2$ . At the end of the feeding, 500  $\mu\text{L}$  of 10% (v/v) KOH as used to stop  $^{14}\text{CO}_2$  generation and capture the residue  $^{14}\text{CO}_2$  in the chamber. The labeled leaf, unlabeled leaves and whole roots of each plant were harvested at 1 h, 7 h and 19 h after labeling.

**Fractionation of  $^{14}\text{CO}_2$ -labelled plant tissue.** Each sample was homogenized in liquid nitrogen, boiled for 10 min in successive 80%, 50%, and 20% (v/v) ethanol, and then separated into the soluble and insoluble fractions by centrifugation. The ethanol insoluble fractions (starch, protein, and cell wall) were digested with amylase and amyloglucosidase (10 U each per 200  $\mu\text{L}$  of insoluble fraction, Roche Biosciences, Indianapolis, IN) to analyze for starch, and digested with pronase (10 U per 200  $\mu\text{L}$  of insoluble fraction, *Streptomyces griseus*, Calbiochem®, Japan) to analyze for protein. The ethanol soluble solutions were fractionated into organic acids, amino acids, and sugars by ion-exchange chromatography using established methods in our lab. The  $^{14}\text{C}$  in each fraction was measured by liquid scintillation counting.

**RNA isolation and quantitative reverse transcription PCR.** Five-week-old plants grown in Hoagland solution (12/12 h day/night, 21/23 °C) were transferred to Hoagland solution containing 200 mM NaCl, 300 mM mannitol for 0, 6, 12, and 24 h. Source leaf was harvested from each plant. Total RNA was extracted from each harvested sample with TRIzol® reagent (Invitrogen, Cansbad, CA). cDNA was synthesized using the high capacity cDNA Reverse Transcription Kit (Applied Biosystems, Vilnius, Lithuania). The primers for *Actin2* (housekeeping gene) amplification were forward, 5'-GGTGATGGTGTGCT-3'; reverse, 5'-ACTGAGC ACAATGTAC-3'. The primers for *SnRK1.1* were forward, 5'-CCGAATTGGGGATAGTCTGAAAATTGC-3'; reverse, 5'-CTCA

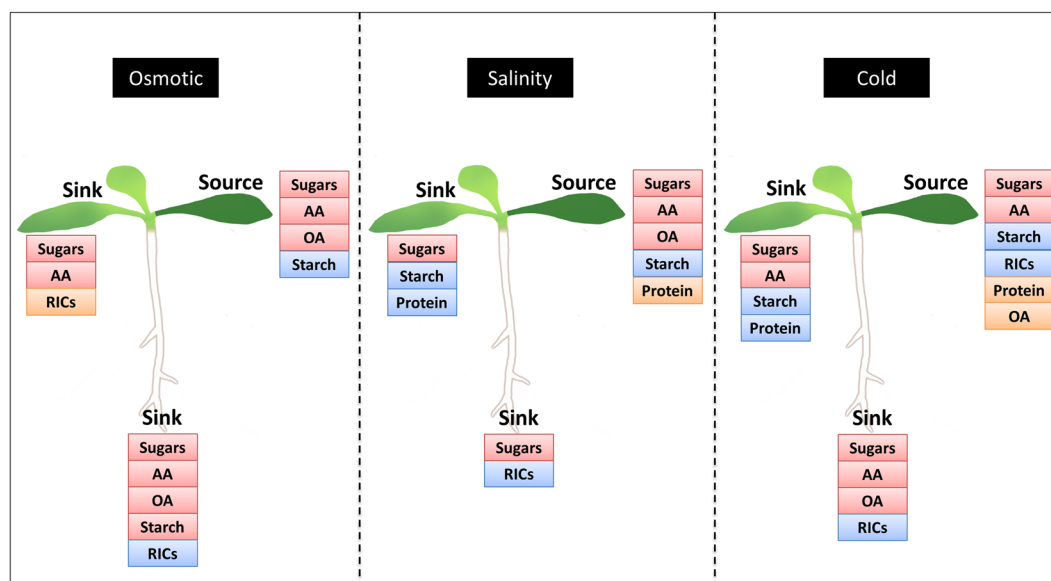


**Figure 8.** A model of the common and specific responses of stress-triggered alterations in metabolite pools. Changes in <sup>14</sup>C partitioning into metabolites by cold (0 °C), 300 mM mannitol, and 200 mM NaCl were compared over the diurnal period. Colored boxes indicate the percentage change in <sup>14</sup>C flow under stress: metabolites in red boxes increased; in blue boxes decreased and metabolites within orange box increased and then decreased ( $p < 0.05$ ) over the 24 h period.

TCTACTCGTTTGAACATGAGAATTTAGCG-3'. The primers for *SnRK1.2* were forward, 5'-GAACTTCAGC TATACAAAGC -3'; reverse, 5'-GCGCATAGATCCAAGAAG-3'. The primers for *AtTPS1* were forward, 5'-GAGCTTAGAGAGAAGAGGAAGAGCAA-3'; reverse, 5'-TTCTAAACGCAAGTCATTCTCAGAGT-3'. The primers for *AtSWEET11* were forward, 5'-TCCTTCTCCTAACAACCTATATACCATG-3', 5'-TCCTATAG AACGTTGGCACAGGA-3'. The primers for *AtAPL3* were forward, 5'-TCAGCACCATGCGATAGTAAAGC-3'; reverse, 5'-CAGTTGGTTTCTCAGAGAAATGGA-3'. Primers were optimized and the efficiency was calculated by making a standard curve with different dilutions of cDNA. One mL of each cDNA was used to amplify in 10 mL PCR reaction containing 2 × ABsolute™ Blue qPCR SYBR Green ROX Mix (ABgene, foster city, CA) and 150 nM primers for genes mentioned above. The real-time PCR was performed in Applied Biosystems 7300 Real-time PCR System (Foster city, CA), the conditions were as follows: 10 min at 95 °C, 15 s at 95 °C, 40 cycles of 15 s at 95 °C, and 1 min at 60 °C. Source leaf from one plant represent one biological replicate. Three technical replicates were performed for each of the 3 biological replicates. ddCt method<sup>76</sup> was used to analyze the expression of each gene based on the fold changes of relative transcripts in experimental sample compared with control sample.

**Statistical analysis.** All tests for significant differences between treatment and control data were done using one-way ANOVA in the R environment. Heatmaps were generated using a web server Heatmapper (<http://www.heatmapper.ca/expression/>).

**Data availability.** All of the materials, data and associated protocols will be made available upon request without preconditions. All data generated from this work, not presented in the figures is in the Supplemental Information file.

## References

1. Taiz, L. & Zeiger, E. *Plant Physiology*. 762–764 (Sinauer Associates, 2010).
2. Smith, A. M. & Stitt, M. Coordination of carbon supply and plant growth. *Plant Cell Environ.* **30**, 1126–1149 (2007).
3. Cross, J. M. *et al.* Variation of enzyme activities and metabolite levels in 24 arabidopsis accessions growing in carbon-limited conditions. *Plant Physiol.* **142**, 1574–1588 (2006).
4. Stitt, M., Gibon, Y., Lunn, J. E. & Piques, M. Multilevel genomics analysis of carbon signalling during low carbon availability: coordinating the supply and utilisation of carbon in a fluctuating environment. *Funct. Plant Biol.* **34**, 526–549 (2007).
5. Sulpice, R. *et al.* Starch as a major integrator in the regulation of plant growth. *Pro. Natl. Acad. Sci. USA* **106**, 10348–10353 (2009).
6. Thalmann, M. & Santelia, D. Starch as a determinant of plant fitness under abiotic stress. *New Phytol.* **214**, 943–951 (2017).
7. Hu, M. Y., Shi, Z. G., Xu, P., Li, H. & Zhang, Z. B. Wheat acclimate to water deficit by modifying carbohydrates metabolism, water use efficiency, and growth. *Braz. J. Bot.* **38**, 505–515 (2015).
8. Cuellar-Ortiz, S. M., Arrieta-Montiel, M. D., Acosta-Gallegos, J. & Covarrubias, A. A. Relationship between carbohydrate partitioning and drought resistance in common bean. *Plant Cell Environ.* **31**, 1399–1409 (2008).
9. Xu, W. *et al.* Drought stress condition increases root to shoot ratio via alteration of carbohydrate partitioning and enzymatic activity in rice seedlings. *Acta Physiol. Plant.* **37** (2015).
10. Wang, Z. C. & Stutte, G. W. The Role of Carbohydrates in Active Osmotic Adjustment in Apple under Water-Stress. *J. Am. Soc. Hortic. Sci.* **117**, 816–823 (1992).
11. Luquet, D. *et al.* Orchestration of transpiration, growth and carbohydrate dynamics in rice during a drydown cycle. *Funct. Plant Biol.* **35**, 689–704 (2008).

12. Wang, X. C. *et al.* Comparative Proteomics of *Thellungiella halophila* Leaves from Plants Subjected to Salinity Reveals the Importance of Chloroplastic Starch and Soluble Sugars in Halophyte Salt Tolerance. *Mol. Cell Proteomics* **12**, 2174–2195 (2013).
13. Yin, Y. G. *et al.* Salinity induces carbohydrate accumulation and sugar-regulated starch biosynthetic genes in tomato (*Solanum lycopersicum* L. cv. 'Micro-Tom') fruits in an ABA- and osmotic stress-independent manner. *J. Exp. Bot.* **61**, 563–574 (2010).
14. Balibrea, M. E., Dell'Amico, J., Bolarin, M. C. & Perez-Alfocea, F. Carbon partitioning and sucrose metabolism in tomato plants growing under salinity. *Physiol. Plant.* **110**, 503–511 (2000).
15. Pattanagul, W. & Thitisaksakul, M. Effect of salinity stress on growth and carbohydrate metabolism in three rice (*Oryza sativa* L.) cultivars differing in salinity tolerance. *Indian J. Exp. Biol.* **46**, 736–742 (2008).
16. Kempa, S. *et al.* A plastid-localized glycogen synthase kinase 3 modulates stress tolerance and carbohydrate metabolism. *Plant J.* **49**, 1076–1090 (2007).
17. Thitisaksakul, M., Arias, M. C., Dong, S. Y. & Beckles, D. M. Overexpression of GSK3-like Kinase 5 (OsGSK5) in rice (*Oryza sativa*) enhances salinity tolerance in part via preferential carbon allocation to root starch. *Funct. Plant Biol.* **44**, 705–719 (2017).
18. Chen, H. J., Chen, J. Y. & Wang, S. J. Molecular regulation of starch accumulation in rice seedling leaves in response to salt stress. *Acta Physiol. Plant.* **30**, 135–142 (2008).
19. Theerawitaya, C., Boriboonkaset, T., Cha-Um, S., Supaibulwatana, K. & Kirdmanee, C. Transcriptional regulations of the genes of starch metabolism and physiological changes in response to salt stress rice (*Oryza sativa* L.) seedlings. *Physiol. Mol. Biol. Plants* **18** (2012).
20. Kaplan, F. & Guy, C. L. RNA interference of *Arabidopsis* beta-amylase8 prevents maltose accumulation upon cold shock and increases sensitivity of PSII photochemical efficiency to freezing stress. *Plant J.* **44**, 730–743 (2005).
21. Hoermiller, I. I. *et al.* Subcellular reprogramming of metabolism during cold acclimation in *Arabidopsis thaliana*. *Plant Cell Environ.* **40**, 602–610 (2017).
22. Kaplan, F. & Guy, C. L. beta-amylase induction and the protective role of maltose during temperature shock. *Plant Physiol.* **135**, 1674–1684 (2004).
23. Sicher, R. Carbon partitioning and the impact of starch deficiency on the initial response of *Arabidopsis* to chilling temperatures. *Plant Sci.* **181**, 167–176 (2011).
24. Yano, R., Nakamura, M., Yoneyama, T. & Nishida, I. Starch-related alpha-glucan/water dikinase is involved in the cold-induced development of freezing tolerance in *Arabidopsis*. *Plant Physiol.* **138**, 837–846 (2005).
25. Nagao, M., Minami, A., Arakawa, K., Fujikawa, S. & Takezawa, D. Rapid degradation of starch in chloroplasts and concomitant accumulation of soluble sugars associated with ABA-induced freezing tolerance in the moss *Physcomitrella patens*. *J. Plant Physiol.* **162**, 169–180 (2005).
26. Henry, C. *et al.* Differential Role for Trehalose Metabolism in Salt-Stressed Maize. *Plant Physiol.* **169**, 1072–1089 (2015).
27. Oury, V. *et al.* Is Change in Ovary Carbon Status a Cause or a Consequence of Maize Ovary Abortion in Water Deficit during Flowering? *Plant Physiol.* **171**, 997–1008 (2016).
28. Kolling, K., Muller, A., Flutsch, P. & Zeeman, S. C. A device for single leaf labelling with CO<sub>2</sub> isotopes to study carbon allocation and partitioning in *Arabidopsis thaliana*. *Plant Methods* **9** (2013).
29. Kolling, K., Thalmann, M., Muller, A., Jenny, C. & Zeeman, S. C. Carbon partitioning in *Arabidopsis thaliana* is a dynamic process controlled by the plants metabolic status and its circadian clock. *Plant Cell Environ.* **38**, 1965–1979 (2015).
30. Durand, M. *et al.* Water Deficit Enhances C Export to the Roots in *Arabidopsis thaliana* Plants with Contribution of Sucrose Transporters in Both Shoot and Roots. *Plant Physiol.* **170**, 1460–1479 (2016).
31. Figueroa, C. M. *et al.* Trehalose 6-phosphate coordinates organic and amino acid metabolism with carbon availability. *Plant J.* **85**, 410–423 (2016).
32. Thalmann, M. *et al.* Regulation of Leaf Starch Degradation by Absciscic Acid Is Important for Osmotic Stress Tolerance in Plants. *Plant Cell* **28**, 1860–1878 (2016).
33. Fernie, A. R., Geigenberger, P. & Stitt, M. Flux an important, but neglected, component of functional genomics. *Curr. Opin. Plant Biol.* **8**, 174–182 (2005).
34. Fernie, A. R. & Morgan, J. A. Analysis of metabolic flux using dynamic labelling and metabolic modelling. *Plant Cell Environ.* **36**, 1738–1750 (2013).
35. Geiger, D. R., Koch, K. E. & Shieh, W. J. Effect of environmental factors on whole plant assimilate partitioning and associated gene expression. *J. Exp. Bot.* **47**, 1229–1238 (1996).
36. Gao, Z. F., Sagi, M. & Lips, S. H. Carbohydrate metabolism in leaves and assimilate partitioning in fruits of tomato (*Lycopersicon esculentum* L.) as affected by salinity. *Plant Sci.* **135**, 149–159 (1998).
37. Yang, J. C., Zhang, J. H., Wang, Z. Q., Xu, G. W. & Zhu, Q. S. Activities of key enzymes in sucrose-to-starch conversion in wheat grains subjected to water deficit during grain filling. *Plant Physiol.* **135**, 1621–1629 (2004).
38. Thitisaksakul, M., Dong, S. & Beckles, D. M. How rice Glycogen Synthase Kinase-like 5 (OsGSK5) integrates salinity stress response to source-sink adaptation: A proposed model. *Plant Signal. Behav.* **12**, e1403708 (2017).
39. Emanuele, S. *et al.* SnRK1 from *Arabidopsis thaliana* is an atypical AMPK. *Plant J.* **82**, 183–192 (2015).
40. Baena-Gonzalez, E., Rolland, F., Thevelein, J. M. & Sheen, J. A central integrator of transcription networks in plant stress and energy signalling. *Nature* **448**, 938–942 (2007).
41. Polge, C. & Thomas, M. SNF1/AMPK/SnRK1 kinases, global regulators at the heart of energy control? *Trends Plant Sci.* **12**, 20–28 (2007).
42. Jossier, M. *et al.* SnRK1 (SNF1-related kinase 1) has a central role in sugar and ABA signalling in *Arabidopsis thaliana*. *Plant J.* **59**, 316–328 (2009).
43. Jamsheer, K. M. & Laxmi, A. Expression of *Arabidopsis* FCS-Like Zinc finger genes is differentially regulated by sugars, cellular energy level, and abiotic stress. *Front. Plant Sci.* **6**, <https://doi.org/10.3389/fpls.2015.00746> (2015).
44. Lawlor, D. W. & Paul, M. J. Source/sink interactions underpin crop yield: the case for trehalose 6-phosphate/SnRK1 in improvement of wheat. *Front. Plant Sci.* **5**, 418, <https://doi.org/10.3389/fpls.2014.00418> (2014).
45. Yu, S. M., Lo, S. F. & Ho, T. H. D. Source-Sink Communication: Regulated by Hormone, Nutrient, and Stress Cross-Signaling. *Trends Plant Sci.* **20**, 844–857 (2015).
46. Avonce, N. *et al.* The *Arabidopsis* trehalose-6-P synthase AtTPS1 gene is a regulator of glucose, abscisic acid, and stress signaling. *Plant Physiol.* **136**, 3649–3659 (2004).
47. Chen, L. Q. *et al.* Sucrose efflux mediated by SWEET proteins as a key step for phloem transport. *Science* **335**, 207–211 (2012).
48. Chen, L. Q. *et al.* Sugar transporters for intercellular exchange and nutrition of pathogens. *Nature* **468**, 527–532 (2010).
49. Baker, R. F., Leach, K. A. & Braun, D. M. SWEET as Sugar: New Sucrose Effluxers in Plants. *Mol. Plant* **5**, 766–768 (2012).
50. Araujo, W. L., Tohge, T., Ishizaki, K., Leaver, C. J. & Fernie, A. R. Protein degradation - an alternative respiratory substrate for stressed plants. *Trends Plant Sci.* **16**, 489–498 (2011).
51. Brouquisse, R., James, F., Raymond, P. & Pradet, A. Study of glucose starvation in excised maize root tips. *Plant Physiol.* **96**, 619–626 (1991).
52. Izumi, M., Hidema, J., Makino, A. & Ishida, H. Autophagy Contributes to Nighttime Energy Availability for Growth in *Arabidopsis*. *Plant Physiol.* **161**, 1682–1693 (2013).
53. Pilkington, S. M. *et al.* Relationship between starch degradation and carbon demand for maintenance and growth in *Arabidopsis thaliana* in different irradiance and temperature regimes. *Plant Cell Environ.* **38**, 157–171 (2015).

54. Ishihara, H., Obata, T., Sulpice, R., Fernie, A. R. & Stitt, M. Quantifying protein synthesis and degradation in Arabidopsis by dynamic <sup>13</sup>C labeling and analysis of enrichment in individual amino acids in their free pools and in protein. *Plant Physiol.* **168**, 74–93 (2015).
55. Hirota, T., Izumi, M., Wada, S., Makino, A. & Ishida, H. Vacuolar Protein Degradation via Autophagy Provides Substrates to Amino Acid Catabolic Pathways as an Adaptive Response to Sugar Starvation in Arabidopsis thaliana. *Plant Cell Physiol.* <https://doi.org/10.1093/pcp/pcy005> (2018).
56. Skirycz, A. *et al.* Developmental stage specificity and the role of mitochondrial metabolism in the response of Arabidopsis leaves to prolonged mild osmotic stress. *Plant Physiol.* **152**, 226–244 (2010).
57. Zanella, M. *et al.* beta-amylase 1 (BAM1) degrades transitory starch to sustain proline biosynthesis during drought stress. *J. Exp. Bot.* **67**, 1819–1826 (2016).
58. Monroe, J. D. *et al.* beta-Amylase1 and beta-amylase3 are plastidic starch hydrolases in Arabidopsis That Seem to Be Adapted for Different Thermal, pH, and stress conditions. *Plant Physiol.* **166**, 1748–1763 (2014).
59. Valerio, C. *et al.* Thioredoxin-regulated beta-amylase (BAM1) triggers diurnal starch degradation in guard cells, and in mesophyll cells under osmotic stress. *J. Exp. Bot.* **62**, 545–555 (2011).
60. Hummel, I. *et al.* Arabidopsis Plants Acclimate to Water Deficit at Low Cost through Changes of Carbon Usage: An Integrated Perspective Using Growth, Metabolite, Enzyme, and Gene Expression Analysis. *Plant Physiol.* **154**, 357–372 (2010).
61. Harb, A., Krishnan, A., Ambavaram, M. M. & Pereira, A. Molecular and physiological analysis of drought stress in Arabidopsis reveals early responses leading to acclimation in plant growth. *Plant Physiol.* **154**, 1254–1271 (2010).
62. Kempa, S., Krasensky, J., Dal Santo, S., Kopka, J. & Jonak, C. A Central Role of Absciscic Acid in Stress-Regulated Carbohydrate Metabolism. *PLoS one* **3**, <https://doi.org/10.1371/journal.pone.0003935> (2008).
63. Stitt, M. & Zeeman, S. C. Starch turnover: pathways, regulation and role in growth. *Curr. Opin. Plant Biol.* **15**, 282–292 (2012).
64. Scialdone, A. *et al.* Arabidopsis plants perform arithmetic division to prevent starvation at night. *elife*. **2**, e00669 (2013).
65. Graf, A., Schlereth, A., Stitt, M. & Smith, A. M. Circadian control of carbohydrate availability for growth in Arabidopsis plants at night. *Proc Natl Acad Sci USA*. **107**, 9458–9463 (2010).
66. Rolland, F., Baena-Gonzalez, E. & Sheen, J. Sugar sensing and signaling in plants: conserved and novel mechanisms. *Annu. Rev. Plant Biol.* **57**, 675–709 (2006).
67. Morkunas, I., Borek, S., Formela, M. & Ratajczak, L. In Carbohydrates - Comprehensive Studies on Glycobiology and Glycotechnology (ed. Chuan-Fa Chang) Ch. 19, 409 (2012).
68. Ceusters, N., Van den Ende, W. & Ceusters, J. Exploration of Sweet Immunity to Enhance Abiotic Stress Tolerance in Plants: Lessons from CAM. *Progress in Botany*. **78**, 145–166 (2016).
69. Koch, K. E. Carbohydrate-Modulated Gene Expression in Plants. *Annu. Rev. Plant Physiol. Plant Mol. Biol.* **47**, 509–540 (1996).
70. Keunen, E., Peshev, D., Vangronsveld, J., Van den Ende, W. & Cuypers, A. Plant sugars are crucial players in the oxidative challenge during abiotic stress: extending the traditional concept. *Plant Cell Environ.* **36**, 1242–1255 (2013).
71. Durand, M. *et al.* Carbon source-sink relationship in Arabidopsis thaliana: the role of sucrose transporters. *Planta* **247**, 587–611 (2018).
72. McKibbin, R. S. *et al.* Production of high-starch, low-glucose potatoes through over-expression of the metabolic regulator SnRK1. *Plant Biotechnol. J.* **4**, 409–418 (2006).
73. Lin, C. R. *et al.* SnRK1A-Interacting Negative Regulators Modulate the Nutrient Starvation Signaling Sensor SnRK1 in Source-Sink Communication in Cereal Seedlings under Abiotic Stress. *The Plant cell* **26**, 808–827 (2014).
74. Williams, S. P., Rangarajan, P., Donahue, J. L., Hess, J. E. & Gillaspay, G. E. Regulation of Sucrose non-Fermenting Related Kinase 1 genes in Arabidopsis thaliana. *Front. Plant Sci.* **5**, <https://doi.org/10.3389/Fpls.2014.00324> (2014).
75. Smith, A. M. & Zeeman, S. C. Quantification of starch in plant tissues. *Nat. Protoc.* **1**, 1342–1345 (2006).
76. Livak, K. J. & Schmittgen, T. D. Analysis of relative gene expression data using real-time quantitative PCR and the 2(-Delta Delta C(T)) Method. *Methods* **25**, 402–408 (2001).

## Acknowledgements

SD thanks the China Scholarship Council, UC Davis Horticulture & Agronomy Graduate Group Scholarship, and the Henry A. Jastro Graduate Research Award for Ph.D. funding. We thank Xiumei Huang, Aaron Krelstein and Nicolaus Nazarenkov for technical assistance. Karin Albornoz, Jessie Bacha, Bixuan Chen and Emma Shipman are acknowledged for their helpful input on the manuscript.

## Author Contributions

D.B. and S.D. conceived the experiment; S.D. designed all experiments, S.D. and J.Z. conducted the experiments, S.D. and D.B. analyzed the results and wrote the manuscript. All authors reviewed the manuscript.

## Additional Information

**Supplementary information** accompanies this paper at <https://doi.org/10.1038/s41598-018-27610-y>.

**Competing Interests:** The authors declare no competing interests.

**Publisher's note:** Springer Nature remains neutral with regard to jurisdictional claims in published maps and institutional affiliations.



**Open Access** This article is licensed under a Creative Commons Attribution 4.0 International License, which permits use, sharing, adaptation, distribution and reproduction in any medium or format, as long as you give appropriate credit to the original author(s) and the source, provide a link to the Creative Commons license, and indicate if changes were made. The images or other third party material in this article are included in the article's Creative Commons license, unless indicated otherwise in a credit line to the material. If material is not included in the article's Creative Commons license and your intended use is not permitted by statutory regulation or exceeds the permitted use, you will need to obtain permission directly from the copyright holder. To view a copy of this license, visit <http://creativecommons.org/licenses/by/4.0/>.

© The Author(s) 2018